J. Phys.: Condens. Matter **22** (2010) 454117 (11pp) doi:10.1088/0953-8984/22/45/454117

Facilitated translocation of polypeptides through a single nanopore

Robert Bikwemu[1], Aaron J Wolfe[1], Xiangjun Xing[2] and Liviu Movileanu[1,3,4,5]

[1] Department of Physics, Syracuse University, 201 Physics Building, Syracuse, NY 13244-1130, USA
[2] Institute of Natural Sciences and Department of Physics, Shanghai Jiao Tong University, Shanghai, 200240, People's Republic of China
[3] Structural Biology, Biochemistry, and Biophysics Program, Syracuse University, 111 College Place, Syracuse, NY 13244-4100, USA
[4] The Syracuse Biomaterials Institute, Syracuse University, 121 Link Hall, Syracuse, NY 13244, USA

E-mail: lmovilea@physics.syr.edu

Received 14 April 2010, in final form 26 August 2010
Published 29 October 2010
Online at stacks.iop.org/JPhysCM/22/454117

Abstract
The transport of polypeptides through nanopores is a key process in biology and medical biotechnology. Despite its critical importance, the underlying kinetics of polypeptide translocation through protein nanopores is not yet comprehensively understood. Here, we present a simple two-barrier, one-well kinetic model for the translocation of short positively charged polypeptides through a single transmembrane protein nanopore that is equipped with negatively charged rings, simply called traps. We demonstrate that the presence of these traps within the interior of the nanopore dramatically alters the free energy landscape for the partitioning of the polypeptide into the nanopore interior, as revealed by significant modifications in the activation free energies required for the transitions of the polypeptide from one state to the other. Our kinetic model permits the calculation of the relative and absolute exit frequencies of the short cationic polypeptides through either opening of the nanopore. Moreover, this approach enabled quantitative assessment of the kinetics of translocation of the polypeptides through a protein nanopore, which is strongly dependent on several factors, including the nature of the translocating polypeptide, the position of the traps, the strength of the polypeptide–attractive trap interactions and the applied transmembrane voltage.

1. Introduction

Although it is well documented that polypeptides traverse transmembrane protein pores [1], the underlying mechanisms that drive the translocation process are poorly understood [2, 3]. The fundamental reason for this problem is the complexity of the free energy landscape for the translocation of polypeptides across a narrow pore in a linear fashion. This is especially true, if we consider the presence of multiple binding sites within the nanopore interior that pull the polypeptides into the pore. This electrostatic pulling of polypeptides is a process that adds to the complexity of the energetic landscape associated with the electrophoretic insertion accomplished by the transmembrane voltage [4–13].

In general, the translocation of polypeptides through protein pores is governed by three distinct mechanisms: (i) the ATP-dependent pulling from the *N*-terminal fragment of the protein, (ii) the electrophoretic-type pulling through applied transmembrane voltage that acts on the positively charged *N*-terminal presequence of the translocating protein, and (iii) the attraction between different regions of the polypeptide and well-defined binding sites located within the pore interior [14]. Recently, several groups have shown that protein translocation across protein pores can also occur in the absence of an ATP-driven mechanism [14–16]. For example, a transmembrane β-barrel pore can serve as a protein tunnel for enzymes to

[5] Address for correspondence: Department of Physics, Syracuse University, 201 Physics Building, Syracuse, NY 13244-1130, USA.

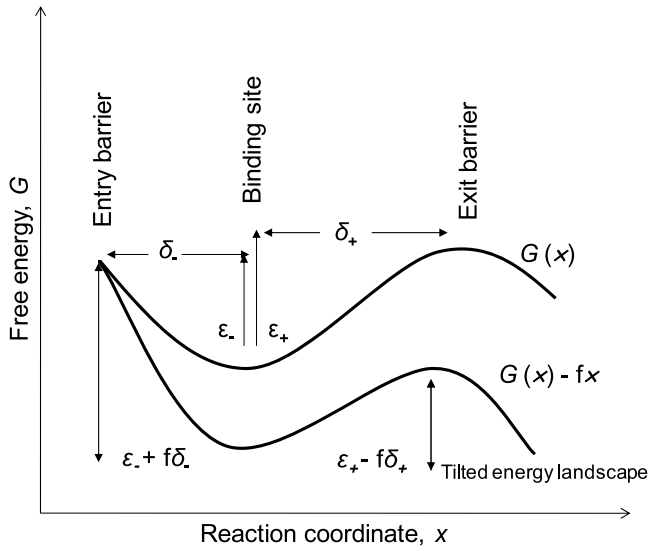

Figure 1. A simple two-barrier, single-well free energy landscape for the translocation of polypeptides through a single wild-type α-hemolysin (WT-αHL) pore [32]. The first and second barrier indicates the entry and exit free energy height, respectively. The top continuous line represents the free energy landscape at zero transmembrane voltage. The bottom continuous line indicates the hypothetical free energy landscape at a transmembrane voltage greater than zero.

enter the cytosol [15, 17]. The complexity of the polypeptide–pore interactions is given by the multitude of protein–protein contacts that can be either electrostatic or hydrophobic in nature. A quantitative understanding of the impact of these cumulative interactions on the overall translocation kinetics and thermodynamics is not yet available.

In this paper, we consider a simple analytical model inspired by protein translocation through mitochondrial membranes [18–22]. We present a qualitative and quantitative description of the kinetic rates of the interaction between short cationic polypeptides and a protein pore equipped with attractive electrostatic traps. The employed experimental parameters were extracted from our prior studies with the *staphylococcal* α-hemolysin (αHL) pore, a heptameric protein of known crystal structure [23]. The traps consisted of rings of negatively charged aspartic acid residues engineered on each subunit of the αHL protein pore [23, 24]. Specifically, the K131D and K147D mutations were accomplished by cassette mutagenesis (figure 1) [25, 26]. We previously performed single-channel recordings with engineered protein pores to better understand the alterations in the signatures of the polypeptide-induced current blockades [23, 27, 28]. In these studies, we examined the exchange of cationic short polypeptides between the bulk aqueous phase and the pore interior of the αHL protein at the single-molecule level. The obvious fundamental advantage of the αHL protein pore is the fact that it lacks obstructing internal loops, such as in the case of other β-barrel protein pores [29–31], enabling the exploration of polypeptide translocation.

These prior experimental explorations have suggested that the kinetic data undergoes a two-barrier, single-well free energy diagram (figure 1) [2, 28, 32]. This free energy profile is highly sensitive to an array of experimental factors and single-molecule experimental design, such as the location of the attractive traps (Tr), the hydrophobic content of the translocating polypeptide (h), the strength of the polypeptide–attractive trap interactions (s) and the applied transmembrane voltage (V). We employed the reaction rate theory to propose a simple kinetic model for the partitioning of short cationic polypeptides into a protein pore [33–35]. This model facilitates qualitative and quantitative predictions of the association and dissociation rate constants $k_{\rm on}$ and $k_{\rm off}$, as well as ways to separate $k_{\rm off}$ into individual rate constants that correspond to the exit through each of the openings of the protein pore ($k_{\rm off}^{\rm trans}$ and $k_{\rm off}^{\rm cis}$) [23, 32]. In previous single-channel studies [23, 32], the reciprocal of $\tau_{\rm on}$ (the mean inter-event interval) was linearly dependent on the polypeptide concentration, whereas $\tau_{\rm off}$ (the dwell time from the histogram of the occupied states) was independent of the polypeptide concentration. Thus, a simple bimolecular interaction between the polypeptide and the protein pore was assumed. The rate constants for association ($k_{\rm on}$) were derived from the slopes of the plots of $1/\tau_{\rm on}$ versus [pept], where [pept] is the peptide concentration in the aqueous phase. The average $k_{\rm off}$ was derived from the averages of $1/\tau_{\rm off}$ for different peptide concentrations.

1.1. A kinetic model of the polypeptide–pore interactions

The kinetic data obtained from single-channel electrical recordings with various trap-containing αHL protein pores and cationic polypeptides [23, 32] can simply be manipulated using a 1D motion along a reaction coordinate x with a free energy $G(x)$. The free energy landscape for the polypeptide–pore interactions can be represented as a two-barrier, and single-well profile [2, 28, 32]. If we consider that $k_-(0)$ and $k_+(0)$ are the voltage-independent rate constants for the backward and forward reactions, respectively (figure 1):

$$k_-(0) = \gamma {\rm e}^{-\frac{\varepsilon_-}{k_{\rm B}T}} \tag{1}$$

$$k_+(0) = \gamma {\rm e}^{-\frac{\varepsilon_+}{k_{\rm B}T}} \tag{2}$$

where γ is the transmission coefficient [33]. $k_{\rm B}$ and T denote the Boltzmann's constant and the absolute temperature, respectively. Here, ε_- and ε_+ indicate the activation free energies for the entry and exit barriers of the pore, respectively. The lines of the free energy landscape represent the profile at zero and greater than zero transmembrane voltages, respectively (figure 1). δ_- and δ_+ indicate the electrical distances from the minimum of the voltage to the transition state of the backward and forward reactions, respectively. At a finite transmembrane voltage, the free energy landscape is tilted to be $G(x) - fx$ (figure 1) [32]. Therefore, the overall reaction rate constant of the polypeptide to exit the transmembrane protein pore is given by the following expression [33]:

$$k(f) = k_-(0){\rm e}^{f\delta_-} + k_+(0){\rm e}^{-f\delta_+}. \tag{3}$$

For a transition rate constant [33]:

$$k_i = k_{i-0} \exp\left(-\frac{\Delta G^{\neq}}{RT}\right) \tag{4}$$

where k_{i-0} is a constant, and $\Delta G^{\neq}$ is the overall activation free energy. For our two-barrier, one-well model, the overall activation free energy has several components, as follows:

$$\Delta G^{\neq} = \Delta G_n - qV - \Delta G_{\text{trap}}. \tag{5}$$

Here, ΔG_n is the native energetic barrier for the WT protein pore (WT-αHL), q is the effective charge of the polypeptide within the voltage drop, V is the transmembrane voltage, and ΔG_{trap} is the alteration of the activation free energy as a result of the attractive trap. The entry and exit traps are engineered at the *trans* opening of the pore and at the *cis* end of the β barrel [23, 28]. Prior experimental data showed that the entry trap has a major impact on the association rate constant k_{on}, but no primary effect on the dissociation rate constant k_{off} (figure 2(B)) [23]. On the other hand, the exit trap has a major impact on the dissociation rate constant k_{off}, but no serious alteration on the dissociation rate constant k_{on} (figure 2(B)) [23]. Therefore, we assume that the engineered traps overlap with the transition states that correspond to entry and exit barriers (figure 1). It is conceivable that the changes in the barrier height made by the entry trap on the entry barrier have little impact on the exit activation free energy. Vice versa, we judge that the alterations made by the exit trap have no major effect on the activation free energy of the entry barrier. The rate constants of association and dissociation will be given by the following expressions:

$$k_{\text{on}} = k_{\text{on}-0} \exp\left(-\frac{\Delta G_n}{RT}\right) \exp\left(\frac{zV}{V_0}\right) \exp\left(\frac{\Delta G_{\text{trap}}^{\text{trans}}}{RT}\right) \tag{6}$$

$$k_{\text{off}}^{\text{trans}} = k_{\text{off}-0}^{\text{trans}} \exp\left(-\frac{\Delta G_n^{\text{trans}}}{RT}\right) \exp\left(-\frac{z^{\text{trans}}V}{V_0}\right) \times \exp\left(\frac{\Delta G_{\text{trap}}^{\text{trans}}}{RT}\right) \tag{7}$$

$$k_{\text{off}}^{\text{cis}} = k_{\text{off}-0}^{\text{cis}} \exp\left(-\frac{\Delta G_n^{\text{cis}}}{RT}\right) \exp\left(\frac{z^{\text{cis}}V}{V_0}\right) \exp\left(\frac{\Delta G_{\text{trap}}^{\text{cis}}}{RT}\right) \tag{8}$$

where

$$V_0 = \frac{RT}{F} = \frac{kT}{e} = 25.6 \text{ mV} \qquad \text{at room temperature} \tag{9}$$

with F and R denoting the Faraday's and gas constants, respectively. From equations (6)–(9), all rates are strongly temperature dependent [28, 36–38]. The association rate constant (k_{on}) is given by the following expression [34]:

$$k_{\text{on}}(h,\ Tr,\ V) = k_{\text{on}}(h,\ Tr,\ 0) \exp\left[\frac{\zeta_{\text{on}}V}{V_0}\right]. \tag{10}$$

Here, ζ_{on} is the effective number of charges of the polypeptide during the association process. The main parameters that alter the kinetic rate constants, the hydropathy index (h), the nature/location of the attractive traps (Tr), and the applied transmembrane voltage (V), are placed in between parenthesis. We found that the association rate constants undergo a single exponential dependence on the applied transmembrane voltage [23, 32, 39]. Fitting the curves $k_{\text{on}}(V)$ with single exponentials, one can obtain the values of $k_{\text{on}}(h,\ Tr,\ 0)$ that correspond to zero transmembrane voltage. In general, the k_{off} rate constants of dissociation for short polypeptides interacting with the αHL protein pore obey to a biphasic behavior with the applied transmembrane voltage [23, 32, 39]. The dissociation rate constant is given by [34]:

$$k_{\text{off}}(h,\ Tr,\ V) = k_{\text{off}}^{\text{trans}}(h,\ Tr,\ 0) \exp\left[-\frac{\zeta_{\text{off}}^{\text{trans}}V}{V_0}\right] + k_{\text{off}}^{\text{cis}}(h,\ Tr,\ 0) \exp\left[\frac{\zeta_{\text{off}}^{\text{cis}}V}{V_0}\right]. \tag{11}$$

Here $k_{\text{off}}^{\text{trans}}(h,\ Tr,\ 0)$ and $k_{\text{off}}^{\text{cis}}(h,\ Tr,\ 0)$ are the dissociation rate constants of the polypeptides through the *trans* and *cis* entrances at 0 mV, respectively. From the fit of the family of experimental curves $k_{\text{off}}(h,\ Tr,\ V)$ that correspond to individual polypeptides, we can obtain the dissociation rate constants to the *cis* and *trans* sides ($k_{\text{off}}^{\text{cis}}(h,\ Tr,\ 0)$, and $k_{\text{off}}^{\text{trans}}(h,\ Tr,\ 0)$) at a transmembrane potential of 0 mV, respectively. In addition, we can obtain the exponential coefficients $\zeta_{\text{off}}^{\text{trans}}$ and $\zeta_{\text{off}}^{\text{cis}}$. Based upon the rate constants of dissociation, we can examine the relative exit frequencies through the *trans* and *cis* sides [32], respectively:

$$n_{\text{exit}}^{\text{trans}}(h,\ Tr,\ V) = \frac{\frac{1}{\tau_{\text{off}}^{\text{trans}}(h,\ Tr,\ V)}}{\frac{1}{\tau_{\text{off}}^{\text{trans}}(h,\ Tr,\ V)} + \frac{1}{\tau_{\text{off}}^{\text{cis}}(h,\ Tr,\ V)}} \tag{12}$$

and

$$n_{\text{exit}}^{\text{cis}}(h,\ Tr,\ V) = \frac{\frac{1}{\tau_{\text{off}}^{\text{cis}}(h,\ Tr,\ V)}}{\frac{1}{\tau_{\text{off}}^{\text{trans}}(h,\ Tr,\ V)} + \frac{1}{\tau_{\text{off}}^{\text{cis}}(h,\ Tr,\ V)}}. \tag{13}$$

Therefore, the total exit frequency through the *trans* and *cis* entrances is given by the following expression:

$$f_{\text{exit}}^{\text{total}} = f_{\text{exit}}^{\text{trans}} + f_{\text{exit}}^{\text{cis}} = \left[n_{\text{exit}}^{\text{trans}}(h,\ Tr,\ V) + n_{\text{exit}}^{\text{cis}}(h,\ Tr,\ V)\right] \times k_{\text{on}}(h,\ Tr,\ V) C_{\text{pept}} \tag{14}$$

where C_{pept} is the peptide concentration in aqueous phase, at the *trans* side of the bilayer. Using Eyring's transition state theory (TST) [52, 53], the rate constants that correspond to 0 mV can be written [40]:

$$k_{\text{on}}(h,\ Tr,\ 0) = \left(\frac{\kappa k_{\text{B}}T}{h}\right) \exp\left[-\frac{\Delta G_{\text{on}}^{\neq}(h,\ Tr,\ 0)}{RT}\right] \tag{15}$$

$$k_{\text{off}}^{\text{trans}}(h,\ Tr,\ 0) = \left(\frac{\kappa k_{\text{B}}T}{h}\right) \exp\left[-\frac{\Delta G_{\text{off}}^{\neq\text{trans}}(h,\ Tr,\ 0)}{RT}\right] \tag{16}$$

$$k_{\text{off}}^{\text{cis}}(h,\ Tr,\ 0) = \left(\frac{\kappa k_{\text{B}}T}{h}\right) \exp\left[-\frac{\Delta G_{\text{off}}^{\neq\text{cis}}(h,\ Tr,\ 0)}{RT}\right]. \tag{17}$$

Here, h is the Planck constant. κ is the transmission coefficient. The activation free energies are also voltage dependent:

$$\Delta G_{\text{on}}^{\neq}(h,\ Tr,\ V) = \Delta G_{\text{on}}^{\neq}(h,\ Tr,\ 0) - \zeta_{\text{on}}RT\frac{V}{V_0} \tag{18}$$

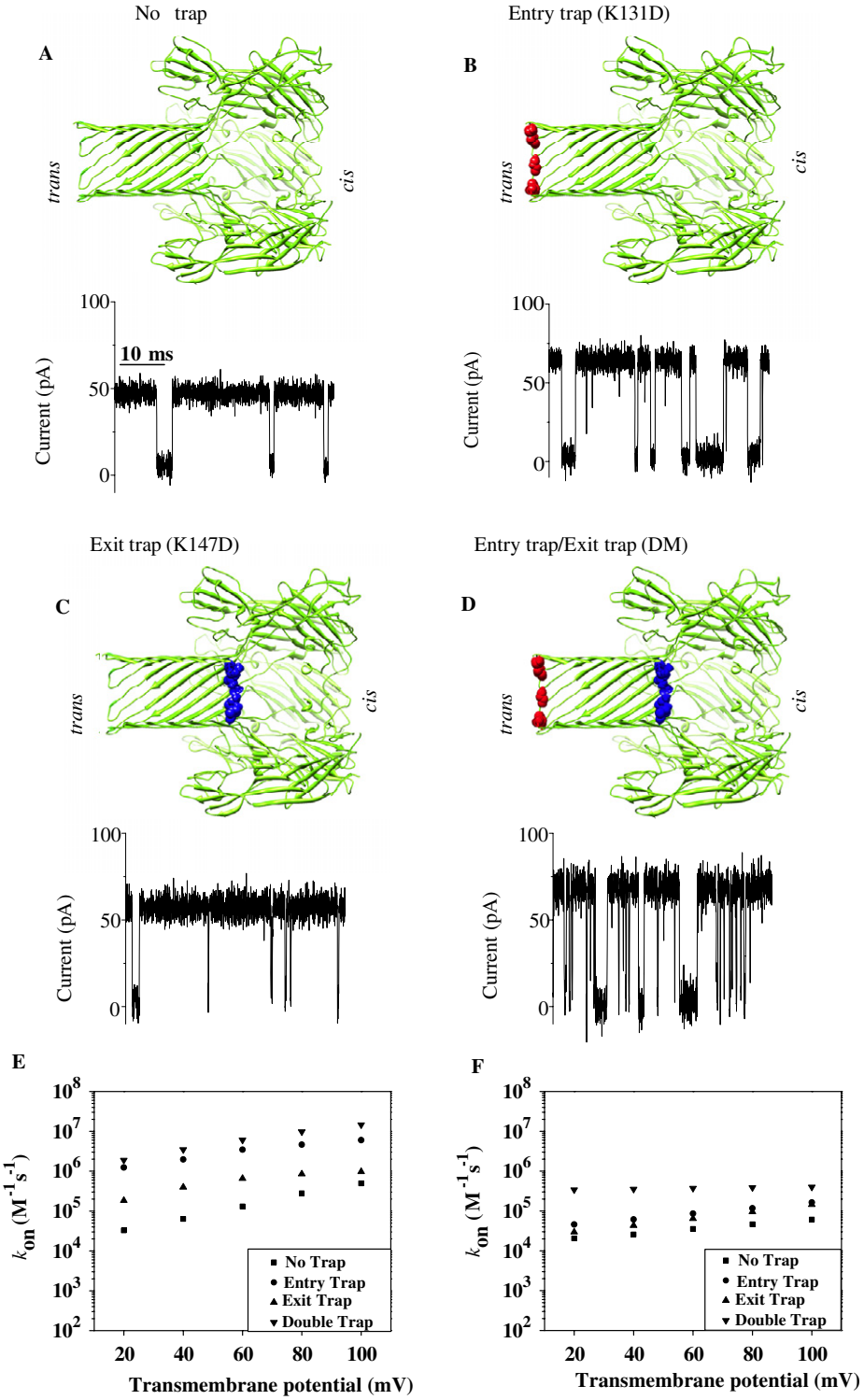

Figure 2. The αHL protein pore was engineered to feature electrostatic traps. The circular traps contained seven aspartic acid residues, one per each subunit of the heptameric αHL pore. (A) No trap, the wild-type αHL (WT-αHL) protein. (B) The entry trap-containing αHL protein (K131D). (C) The exit trap-containing αHL protein (K147D). (D) The double trap-containing αHL protein (DM). The bottom panels show patches of single-channel electrical traces acquired with 34 μM of hydrophilic Syn B2 polypeptide added to the *trans* side of the chamber [23]. The frequency and duration of the polypeptide-induced current blockades were dependent on the position of the engineered attractive trap. All traces were recorded in symmetrical buffer conditions (1 M KCl, 10 mM potassium phosphate, pH 7.4) at a transmembrane voltage of +60 mV. The single-channel electrical traces were low-pass Bessel filtered at 2 kHz. (E) Voltage dependence of the association rate constant k_{on} measured with wild-type and trap-containing αHL pores interacting with the hydrophilic polypeptide Syn B2. (F) The same as in (E), but interacting with the less hydrophilic polypeptide Cox IV.

(This figure is in colour only in the electronic version)

$$\Delta G_{\text{off}}^{\neq \text{trans}}(h,\ Tr,\ V) = \Delta G_{\text{off}}^{\neq \text{trans}}(h,\ Tr,\ 0) + \zeta_{\text{off}}^{\text{trans}} RT \frac{V}{V_0} \quad (19)$$

$$\Delta G_{\text{off}}^{\neq \text{cis}}(h,\ Tr,\ V) = \Delta G_{\text{off}}^{\neq cis}(h,\ Tr,\ 0) - \zeta_{\text{off}}^{\text{cis}} RT \frac{V}{V_0}. \quad (20)$$

If we consider the Eyring 'frequency factor' [34]:

$$\text{ff} = \frac{k_{\text{B}}T}{h} = 6 \times 10^{12}\ \text{s}^{-1}. \quad (21)$$

Then, we can calculate $\Delta G_{\text{on}}(h,\ Tr,\ 0)$, $\Delta G_{\text{off}}^{\text{trans}}(h,\ Tr,\ 0)$ and $\Delta G_{\text{off}}^{\text{cis}}(h,\ Tr,\ 0)$. However, ff from equation (21) is valid for only elementary transitions over a distance less than the mean free path of 0.1 Å. Therefore, we chose the more suitable value of $10^9\ \text{s}^{-1}$, which corresponds to diffusional transitions over a distance of 1 nm [34].

2. Results

The aspartic acid-based traps were engineered by single-site mutagenesis [23, 27]. The polypeptides used in this work were Syn B2 = MLSRQQSQRQSRQQSQRQSRYLL (hydrophilic polypeptide with the hydropathy index $h = -44.4$) and Cox IV = MLSLRQSIRFFKPATRTLCSSRY (much less hydrophilic polypeptide with $h = -5.2$). Electrical recordings were carried out with planar bilayer lipid membranes [41–43]. The electrolyte in both chambers was 1 M KCl, 10 mM potassium phosphate, pH 7.4. The narrowest region of the αHL pore features a β-barrel structure, which forms the transmembrane domain, and is almost 50 Å long and about 20 Å wide (based on side chain to side chain dimensions) (figure 2). The length of the polypeptides in extended conformation is greater than 70 Å. The total internal volume of the β-barrel is about 10^4 Å^3 [44]. The polypeptides were added to the *trans* side of the bilayer chamber.

The time constants τ_{on} and τ_{off} were derived from standard dwell time histograms of the single-channel electrical data [23, 28]. The fits of the data were accomplished using log likelihood ratio (LLR) tests to compare various fitting models [44–46]. In general, the fit of the dwell time histograms contained a well-defined single- or double-exponential function. At a confidence level of 0.95, fits to a three-exponential model were not statistically better than single- or double-exponential models, as judged by the LLR value. As in a previously published report [32], we attributed the very short τ_{off} component to collisions between polypeptides and the entrance of the nanopore. The long τ_{off} component was attributed to major partitioning of polypeptides into the lumen of the nanopores. We employed equation (11) and the voltage dependence of the long τ_{off} to extract the model parameters. Indeed, we found that the dwell time (τ_{off}) of the polypeptides within the pore interior has a biphasic voltage dependence [23, 32]. The U-shaped voltage dependence of the rate constant k_{off} on the transmembrane voltage indicates that the short cationic polypeptides bind to the αHL pore and exit through either the *trans* or *cis* opening. At lower transmembrane voltages, τ_{off} increased with the applied transmembrane voltage, whereas at higher transmembrane voltages, τ_{off} decreased with the applied transmembrane voltage [23, 32]. This finding is specific to semi-flexible charged polypeptides, whose contour length is comparable with the length of the pore.

In figure 2, we show the fundamental dissimilarities between the fourth situations analyzed in this paper: the wild-type pore (figure 2(A), no attractive trap was engineered), the entry trap-containing pore (figure 2(B), a single attractive trap was engineered at the entry of the pore; position 131 near the *trans* opening), the exit trap-containing pore (figure 2(C), a single attractive trap was engineered at the exit of the pore; position 147 near the *cis* end of the barrel), and double trap-containing pore (figure 2(D), this protein pore contains both traps from figures 2(B) and (C)). The association rate constants are shown as family of 2D plots, whose 'x' axes are the applied transmembrane voltages (figures 2(E) and (F)). In particular, figures 2(E) and (F) show the k_{on} values that correspond to a hydrophilic polypeptide (Syn B2) and a less hydrophilic polypeptide (Cox IV), respectively. Clearly, not only the applied transmembrane voltage, but also the nature of the attractive trap and interacting polypeptide strongly impact the rate constant of association. We found a single exponential dependence of k_{on} on the applied transmembrane voltage, confirming that at a transmembrane voltage greater than zero, the free energy landscape is tilted linearly by $G(V)$–fV, where V, the applied transmembrane voltage, is the reaction coordinate [32]. This finding is also in agreement with our simplistic model for which the activation free energy is voltage dependent (see equations (3)–(5)). Remarkably, the k_{on} association rate constant increased dramatically when both the entry and exit traps were present in the pore regardless of the hydrophilic nature of the polypeptide (figures 2(E) and (F)). Moreover, the k_{on} values for the hydrophilic polypeptide were always greater than those obtained for the less hydrophilic polypeptide, confirming a higher energetic penalty for more hydrophobic polypeptides to traverse the pore.

Similarly, the $k_{\text{off}}^{\text{trans}}$ and $k_{\text{off}}^{\text{cis}}$ dissociation rate constants were strongly dependent on not only the applied transmembrane voltage, but also on the location of the electrostatic trap and Kyte–Doolittle hydropathy index of the translocating polypeptide (figure 3) [47]. For example, the entry trap reduced the $k_{\text{off}}^{\text{trans}}$ dissociation rate constant by comparison with the wild-type pore (figures 3(A) and (B)). In contrast, the exit trap greatly increased the $k_{\text{off}}^{\text{cis}}$ dissociation rate constant, suggesting that this modification of the pore catalyzes the transit of the polypeptides from one side of the membrane to the other (figures 3(C) and (D)).

Using equations (12)–(14), we calculated the relative and absolute exit frequencies through either the *trans* or *cis* opening of the pore. We assumed a linear dependence of the native activation free energies $\Delta G_{\text{on}}^{\neq}$, $\Delta G_{\text{off}}^{\text{trans}\neq}$ and $\Delta G_{\text{off}}^{\text{cis}\neq}$ on the Kyte–Doolittle hydropathy index of the translocating polypeptide [47, 48]. This is motivated by the fact that the semi-flexible polypeptides are short enough to implement the linear approximation [49]. For this calculation, we also considered that the electric charges and the hydrophobic units are uniformly distributed along the polypeptide chain. Based on the fitting parameters derived from our previous

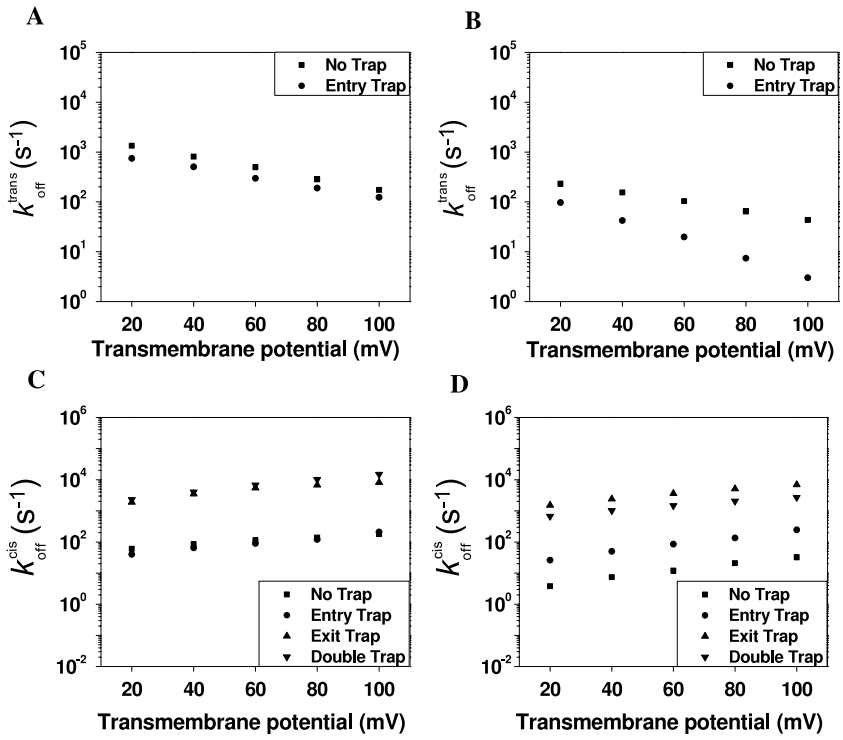

Figure 3. Voltage dependence of the rate constants of dissociation k_{off}^{cis} and k_{off}^{trans} measured with wild-type and trap-containing α HL pores. (A) k_{off}^{trans} measured with the hydrophilic polypeptide Syn B2; (B) k_{off}^{trans} measured with the less hydrophilic polypeptide Cox IV; (C) k_{off}^{cis} measured with the hydrophilic polypeptide Syn B2; (D) k_{off}^{cis} measured with the less hydrophilic polypeptide Cox IV. The other experimental conditions are the same as those showed in figure 2.

experimental data [23, 28], we calculated the relative and absolute exit frequencies as functions depending on the hydropathy index. These kinetic parameters are illustrated as 2D plots of varying applied transmembrane voltage (figures 4 and 5). The data are calculated for the wild-type (figures 4(A), (C), 5(A) and (C)) and entry trap-containing protein pore (figure 4(B), (D), 5(B) and (D)). Increasing the applied transmembrane voltage increases the activation free energy for the dissociation events through the *trans* side, but decreases the activation free energy for the dissociation events through the *cis* side (figure 1). Therefore, the relative *trans* exit frequencies decrease with the applied transmembrane voltage (figures 4(A) and (B)), whereas the relative *cis* exit frequencies increase with the applied transmembrane voltage (figures 4(C) and (D)).

On the other hand, the Kyte–Doolittle hydropathy index has a more complex impact on the dissociation events. For the wild-type protein pore, more hydrophobic polypeptides exhibited a greater relative *trans* exit frequencies than more hydrophilic polypeptides (figure 4(A)). This finding contrasted with that for the entry trap-containing protein pore for which more hydrophilic polypeptides showed an increased relative *trans* exit frequencies as compared to the values obtained with the less hydrophilic polypeptides (figure 4(B)). In the case of the wild-type protein pore, the absolute *trans* and *cis* exit frequencies increased with the applied transmembrane voltage (figures 5(A) and (C)).

In the case of the entry trap-containing protein pore, the effect of the hydropathy index on the absolute exit frequencies was strongly voltage dependent (figures 5(B) and (D)). For example, the short cationic polypeptides exhibited higher absolute *cis* exit frequencies at greater transmembrane voltages (>70 mV), but lower absolute *cis* exit frequencies at low transmembrane voltages (<70 mV) (figure 5(D)). Absolute *trans* exit frequencies increased with the transmembrane voltage for hydrophilic polypeptides ($h \sim 40$), contrasting with their decrease with the transmembrane voltage for less hydrophilic polypeptides ($h \sim -5$) (figure 5(B)). These findings indicate the complexity of the simultaneous impact of the applied transmembrane voltage and the Kyte–Doolittle hydropathy index on the activation free energies required for the polypeptide translocation across the entry trap-containing protein pore.

We calculated the changes in the activation free energies when the property of either the translocating polypeptide (e.g., the Kyte–Doolittle hydropathy index) or the pore (e.g., the location of the traps, the applied transmembrane voltage) was altered. The 'on' activation free energy $\Delta G_{on}^{\neq}$ was always smaller that the 'off' activation free energies $\Delta G_{off}^{trans\neq}$ and $\Delta G_{off}^{cis\neq}$. Table 1 lists the values of these barriers, which were calculated at zero transmembrane voltage. The range of the barrier heights was between 3.9 and 10 kcal mol^{-1}. Both the 'on' and 'off' values were smaller when the entry and exit traps were present within the pore interior. We were interested in exploring the overall effect of the entry and exit traps on the $\Delta G_{off}^{cis\neq}$ activation free energy. Figure 6 shows $\Delta\Delta G_{trap}^{cis} = \Delta G_{off-trap,h}^{cis\neq} - \Delta G_{off-WT,h}^{cis\neq}$, which was calculated at +60 mV. This figure illustrates the effect of the traps on the $\Delta G_{off}^{cis\neq}$ activation free energy for the three types of engineered

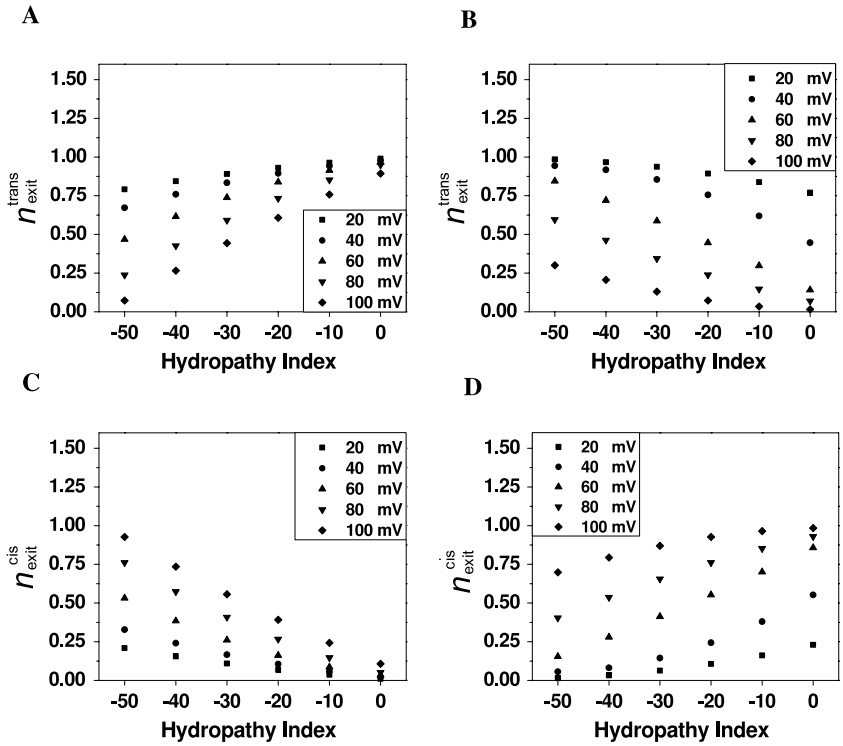

Figure 4. A 2D plot that shows the dependence of the relative exit frequencies as functions of the applied transmembrane voltage and the Kyte–Doolittle hydropathy index. (A) Relative *trans* exit frequency calculated for the WT-αHL protein pore. (B) Relative *trans* exit frequency calculated for the entry trap-containing αHL protein pore. (C) Relative *cis* exit frequency calculated for the WT-αHL protein pore. (D) Relative *cis* exit frequency calculated for the entry trap-containing αHL protein pore.

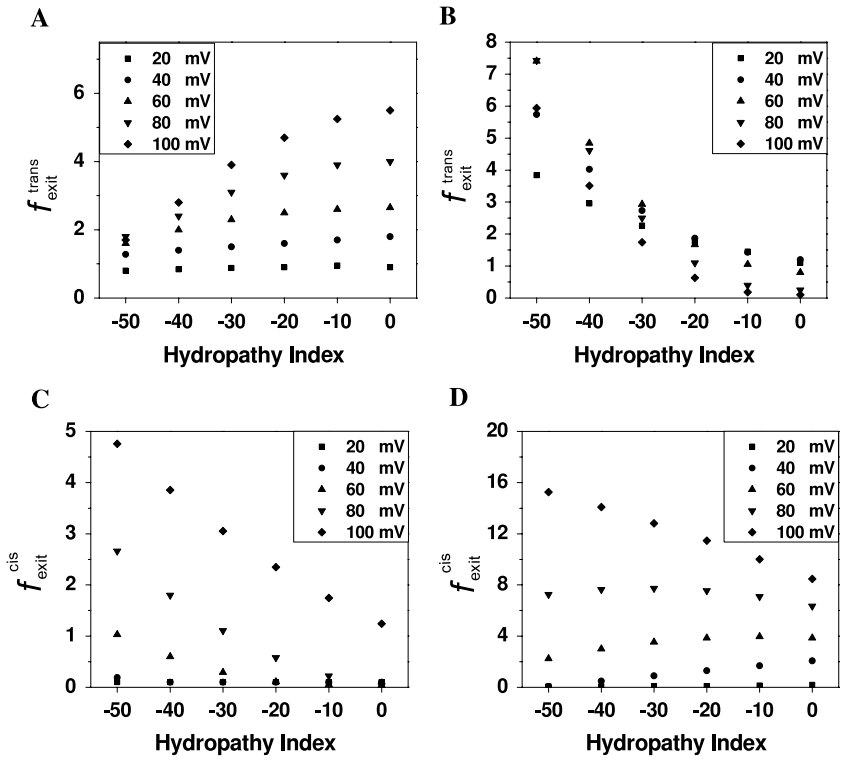

Figure 5. A 2D plot that shows the dependence of the absolute exit frequencies as functions of the applied transmembrane voltage and the Kyte–Doolittle hydropathy index. (A) Absolute *trans* exit frequency calculated for the WT-αHL protein pore. (B) Absolute *trans* exit frequency calculated for the entry trap-containing αHL protein pore. (C) Absolute *cis* exit frequency calculated for the WT-αHL protein pore. (D) Absolute *cis* exit frequency calculated for the entry trap-containing αHL protein pore.

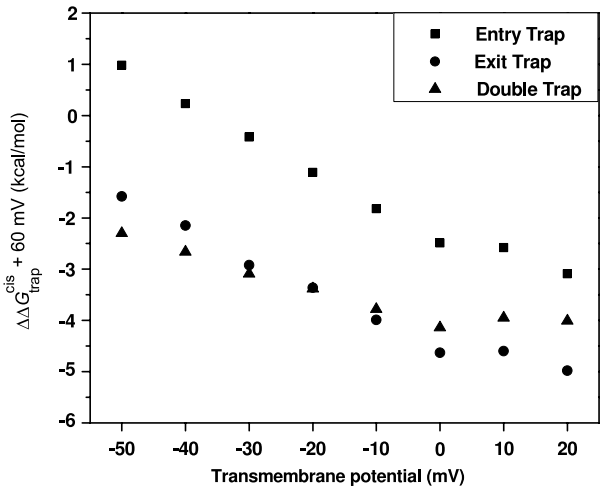

Figure 6. $\Delta\Delta G^{cis}_{trap} = \Delta G^{cis\neq}_{off-trap,h} - \Delta G^{cis\neq}_{off-WT,h}$ calculated at +60 mV. The values used to calculate $\Delta G^{cis}_{off-pore,h}$, where h is the Kyte–Doolittle hydropathy index, were derived from the kinetic rate constants (equations (15)–(21)).

Table 1. The activation free energies $\Delta G^{\neq}_{on}$, $\Delta G^{trans\neq}_{off}$, $\Delta G^{cis\neq}_{off}$, which were calculated at 0 mV. The kinetic rate constants of dissociation were calculated by fitting experimental data with a double-exponential function, where the corresponding kinetic rate constants at 0 mV were extrapolated. (Note: NA—these values could not be determined precisely from fittings.)

Pore/polypeptide	$\Delta G^{\neq}_{on}$ (kcal mol^{-1})	$\Delta G^{trans\neq}_{off}$ (kcal mol^{-1})	$\Delta G^{cis\neq}_{off}$ (kcal mol^{-1})
WT-αHL:SynB2	6.7	7.7	10.0
WT-αHL:Cox IV	6.5	8.9	9.4
K147D:Syn B2	5.1	NA	8.4
K147D:Cox IV	6.5	NA	8.3
DM:SynB2	3.9	NA	8.1
DM:Cox IV	4.9	NA	8.6

nanopores: entry trap-, exit trap-, and double trap (DM)-containing protein pores, respectively. The horizontal axis is the Kyte–Doolittle hydropathy index.

The obvious finding of these calculations is that the reduction in the $\Delta G^{cis\neq}_{off}$ activation free energy is much greater for hydrophobic polypeptides than for hydrophilic polypeptides (figure 6). For example, $\Delta\Delta G^{cis}_{trap} \sim -5$ kcal mol^{-1} for the exit trap-containing protein pores traversed by a hydrophobic polypeptide (hydropathy index $h = 20$), but this value is much smaller than that value corresponding to a hydrophilic polypeptide (hydropathy index $h = -50$). For example, for a hydrophilic polypeptide with $h = -50$, $\Delta\Delta G^{cis}_{trap} \sim -1.5$ and ~ -2.3 kcal mol^{-1} for the exit trap- and double trap-containing protein pores, respectively (figure 6). As expected, the presence of the entry trap within the interior of the pore had a smaller impact than that of exit trap, which overlaps with the transition state corresponding to the exit barrier. Therefore, we infer that the exit trap has a major impact on the ΔG^{cis}_{off} activation free energy and that the hydrophobic polypeptides have a greater ability to exit the pore through the *cis* side than the hydrophilic polypeptides.

3. Discussion

In this paper, we show a simple model that confirms qualitatively our previously published single-channel electrical recordings with engineered protein nanopores interacting with short cationic polypeptides [23, 28]. We judge that this model is only applicable to semi-flexible polypeptides, whose contour length is comparable with the length of the protein pore. For much longer polypeptides, the energetic barrier to traverse the protein pore would be greatly enhanced, decreasing the probability of the translocation events from one side of the membrane to the other. Indeed, our similar single-channel experiments with trap-containing protein pores interacting with folded protein domains provided results that contrast the outcomes of this work [27]. We employed engineered polypeptides of varying positively charged pb_2 presequence of the cytochrome b_2, which were fused to the small RNase barnase (Ba). We tested the interactions of the folded pb_2-Ba polypeptides with the trap-containing protein pores and found that such protein analytes cannot traverse the nanopore from one side of the membrane to the other. For example, the pb_2-Ba polypeptides were locked within the nanopore interior for very long time [27]. This result resembles with the spontaneous attachment of a single folded protein within the interior of a nanopore [50].

Bayley and colleagues, using a similar approach, were able to dramatically increase the k_{on} rate constant of association between single-stranded polynucleotides (ssDNA) and the αHL protein pore equipped with positively charged traps, catalyzing the interaction of nucleic acids with the protein [51]. In contrast with the findings of our work, their single-channel electrical recordings did not show significant alterations in the transit time of the ssDNA polymers through the pore. This dissimilarity can be explained in terms of the features of the translocating polymers [23, 28, 51]. First, an obvious distinction is that ssDNA employed in their work was much longer than length of the nanopore. Second, one difference is the high charged density of the ssDNA due to the phosphate groups as compared to the short cationic polypeptides used previously [23, 28]. Undoubtedly, more experimentation and biophysical computation is required to decipher the underlying mechanisms that govern the translocation of short semi-flexible polymers through nanopores equipped with engineered electrostatic traps.

We interpret that the electrostatic trap implies an additional minimum (i.e., binding site) in the free energy landscape. We judge that for a system containing two binding sites (i.e., two minima), there are two possibilities: (i) the minima and the transition states in the free energy landscape are far away from each other. In this case, they have an independent contribution to the overall kinetics, and (ii) the minima and the transition states are near to each other, so the transition state with the higher energetic barrier reduces, resulting in a faster rate constant for the polypeptide to exit the pore. In agreement with our hypothesis, the exit trap produced a significant increase in the rate constant of dissociation k^{cis}_{off} (figures 3(C) and (D)), altering the exit barrier on the *cis* side of

the barrel (figure 1). For the double trap-containing pore, there are two minima that correspond to the entry and exit traps and one minimum that corresponds to the native binding site, near the pore constriction (figure 1) [32]. Overall, both electrostatic traps increased both the rate constants of association and dissociation, k_{on} and k_{off}, respectively (figures 2(E) and 3).

Our kinetic model predicts that a more hydrophobic polypeptide exhibits a smaller exit activation free energy on the *cis* end of the barrel (figure 6). This result is quite interesting, since it demonstrates that a hydrophobic polymer experiences a lower energetic penalty to exit an aqueous nanopore than a hydrophilic polymer. This finding can be explained in terms of polymer–pore wall interactions, which are mediated by water molecules. The hydrophobic polypeptide shows a repulsive interaction with the pore walls as compared to the hydrophilic polypeptide. Therefore, this model indicates that repulsive interactions can also be employed to increase the rate of translocation from one side of the membrane to the other. An optimized rate of translocation would imply a combination of attractive and repulsive traps. Using stochastic site-binding analytical models, Kolomeisky and his colleagues explored the impact of the binding sites, their nature (e.g., attraction, repulsion) and the asymmetry of the interacting potential on the rate of flow of particles through a nanopore [8, 11]. Remarkably, they found that the attractive binding sites can catalyze the transport at low concentrations in the chamber, contrasting to the situation of high particle concentrations in the chamber where the repulsive binding sites yield the most optimal transport rates.

It is conceivable that polypeptide translocation through barrel-like protein nanopores, which occurs in the outer membranes of mitochondria, chloroplasts and Gram-negative bacteria, undergoes a complex array of attractive and repulsive forces, involving hydrophobic and electrostatic interactions between the side chains of the translocating polypeptide and the side chains of the pore interior. For example, the lethal factor (LF) translocates through the protective antigen channel (PA_{63}) of anthrax toxin in the absence of any ATP-based machinery. In addition of electrostatic interactions between the positively charged residues of the LF polypeptide and acidic side chains of the heptameric pore interior of PA_{63}, this translocation process is also mediated by hydrophobic contacts with a phenylalanine ring located within the pore lumen (14). Collier and colleagues, based upon single-site mutagenesis of this phenylalanine ring, have proposed that the hydrophobic interactions have a major impact in the unfolding of the LF polypeptide, producing a 'translocation competent' conformation. This process catalyzes the polypeptide transport from one side of the membrane to the other. Using a similar approach of our work [23, 27, 28], Guan and colleagues used the αHL protein pore to explore the interactions of aromatic residue-containing polypeptides with nanopores equipped with hydrophobic side chains [52]. This study showed the strength of the hydrophobic interactions that dominate the polypeptide–pore energetic landscape, revealing alterations in the association and dissociation rate constants.

Since the αHL pore maintains the open state for long periods even in extreme experimental conditions (e.g., pH, salt, temperature etc) (3), it should be possible to examine the interaction between unfolded peptides and the lumen of the αHL pore. We cannot say whether the polypeptides undergo conformational transitions when they enter the interior of the αHL pore, but the uniform current blockades suggest that single conformations are adopted within the pore. Chemical denaturants or temperature ramps could be used to determine the associated enthalpy and entropy changes. A fundamental issue that will be addressed in the future experiments is whether the polypeptides bind to the αHL pore in folded, partially folded or unfolded conformations. Of course, more computation and theory is required to determine the limits of existing electrical recording instrumentation for probing subtle conformational changes of the translocating polypeptide [11, 12, 39, 53–58]. On the other hand, larger monomeric β-barrel pores, with the internal diameter greater than that of the αHL protein pore, are desirable for the exploration of the translocation of polypeptides and folded protein domains. These studies require robust, versatile and tractable barrel protein scaffolds that will be used further to engineer functional groups needed in protein translocation.

In summary, we show a simple two-barrier, one-well energetic landscape for obtaining the detailed kinetic profile of polypeptide translocation through a protein nanopore equipped with attractive electrostatic traps. The model parameters are extracted from fittings of experimental kinetic data, derived from prior single-channel recordings, reinforcing the quantitative feature of the model. This work is only applicable to short semi-flexible polypeptides, whose contour length is comparable with the length of the pore. Qualitatively, this study shows that the position of the electrostatic traps, the nature of the translocating polypeptide and transmembrane voltage have a complex impact on the absolute rates for exiting the nanopore. Moreover, the model predicts that the association rate constants decrease with the increase in the hydrophobic content of the translocating polypeptide, in agreement with previously published experimental data [23]. In contrast, the dissociation rate constant across the *cis* end of the barrel increases due to repulsive interactions between the polypeptide and the pore walls, decreasing the activation free energy for exiting the nanopore.

Acknowledgments

We thank Dmitrii Makarov and Anatoly Kolomeisky for stimulating discussions. This work was supported in part by the National Science Foundation (DMR-0706517 and DMR-1006332), the National Institutes of Health (R01 GM088403) and by the Syracuse Biomaterials Institute. RB is a recipient of a fellowship provided by the AGEP-NY-PR Program, which was funded through the National Science Foundation (HRD-0703452).

References

[1] Wickner W and Schekman R 2005 Protein translocation across biological membranes *Science* **310** 1452–6
[2] Movileanu L 2008 Squeezing a single polypeptide through a nanopore *Soft Matter* **4** 925–31

[3] Movileanu L 2009 Interrogating single proteins through nanopores: challenges and opportunities *Trends Biotechnol.* **27** 333–41

[4] Berezhkovskii A M, Pustovoit M A and Bezrukov S M 2002 Effect of binding on particle number fluctuations in a membrane channel *J. Chem. Phys.* **116** 6216–20

[5] Dagdug L, Berezhkovskii A, Bezrukov S M and Weiss G H 2003 Diffusion-controlled reactions with a binding site hidden in a channel *J. Chem. Phys.* **118** 2367–73

[6] Berezhkovskii A M and Bezrukov S M 2005 Optimizing transport of metabolites through large channels: molecular sieves with and without binding *Biophys. J.* **88** L17–9

[7] Berezhkovskii A M, Hummer G and Bezrukov S M 2006 Identity of distributions of direct uphill and downhill translocation times for particles traversing membrane channels *Phys. Rev. Lett.* **97** 020601

[8] Kotsev S and Kolomeisky A B 2006 Effect of orientation in translocation of polymers through nanopores *J. Chem. Phys.* **125** 084906

[9] Krasilnikov O V, Rodrigues C G and Bezrukov S M 2006 Single polymer molecules in a protein nanopore in the limit of a strong polymer–pore attraction *Phys. Rev. Lett.* **97** 018301

[10] Bauer W R and Nadler W 2006 Molecular transport through channels and pores: effects of in-channel interactions and blocking *Proc. Natl Acad. Sci. USA* **103** 11446–51

[11] Kolomeisky A B 2007 Channel-facilitated molecular transport across membranes: attraction, repulsion, and asymmetry *Phys. Rev. Lett.* **98** 048105

[12] Kolomeisky A B and Kotsev S 2008 Effect of interactions on molecular fluxes and fluctuations in the transport across membrane channels *J. Chem. Phys.* **128** 085101

[13] Kotsev S and Kolomeisky A B 2007 Translocation of polymers with folded configurations across nanopores *J. Chem. Phys.* **127** 185103

[14] Krantz B A *et al* 2005 A phenylalanine clamp catalyzes protein translocation through the anthrax toxin pore *Science* **309** 777–81

[15] Krantz B A, Finkelstein A and Collier R J 2006 Protein translocation through the anthrax toxin transmembrane pore is driven by a proton gradient *J. Mol. Biol.* **355** 968–79

[16] Fischer A and Montal M 2007 Single molecule detection of intermediates during botulinum neurotoxin translocation across membranes *Proc. Natl Acad. Sci. USA* **104** 10447–52

[17] Karginov V A, Nestorovich E M, Moayeri M, Leppla S H and Bezrukov S M 2005 Blocking anthrax lethal toxin at the protective antigen channel by using structure-inspired drug design *Proc. Natl Acad. Sci. USA* **102** 15075–80

[18] Huang S, Ratliff K S and Matouschek A 2002 Protein unfolding by the mitochondrial membrane potential *Nat. Struct. Biol.* **9** 301–7

[19] Huang S, Ratliff K S, Schwartz M P, Spenner J M and Matouschek A 1999 Mitochondria unfold precursor proteins by unraveling them from their N-termini *Nat. Struct. Biol.* **6** 1132–8

[20] Prakash S and Matouschek A 2004 Protein unfolding in the cell *Trends Biochem. Sci.* **29** 593–600

[21] Shariff K, Ghosal S and Matouschek A 2004 The force exerted by the membrane potential during protein import into the mitochondrial matrix *Biophys. J.* **86** 3647–52

[22] Inobe T, Kraut D A and Matouschek A 2008 How to pick a protein and pull at it *Nat. Struct. Mol. Biol.* **15** 1135–6

[23] Wolfe A J, Mohammad M M, Cheley S, Bayley H and Movileanu L 2007 Catalyzing the translocation of polypeptides through attractive interactions *J. Am. Chem. Soc.* **129** 14034–41

[24] Mohammad M M and Movileanu L 2010 Impact of distant charge reversals within a robust beta-barrel protein pore *J. Phys. Chem.* B **114** 8750–9

[25] Howorka S *et al* 2000 A protein pore with a single polymer chain tethered within the lumen *J. Am. Chem. Soc.* **122** 2411–6

[26] Movileanu L, Howorka S, Braha O and Bayley H 2000 Detecting protein analytes that modulate transmembrane movement of a polymer chain within a single protein pore *Nat. Biotechnol.* **18** 1091–5

[27] Mohammad M M, Prakash S, Matouschek A and Movileanu L 2008 Controlling a single protein in a nanopore through electrostatic traps *J. Am. Chem. Soc.* **130** 4081–8

[28] Mohammad M M and Movileanu L 2008 Excursion of a single polypeptide into a protein pore: simple physics, but complicated biology *Eur. Biophys. J.* **37** 913–25

[29] van den Berg B 2005 The FadL family: unusual transporters for unusual substrates *Curr. Opin. Struct. Biol.* **15** 401–7

[30] Biswas S, Mohammad M M, Patel D R, Movileanu L and van den Berg B 2007 Structural insight into OprD substrate specificity *Nat. Struct. Mol. Biol.* **14** 1108–9

[31] Biswas S, Mohammad M M, Movileanu L and van den Berg B 2008 Crystal structure of the outer membrane protein OpdK from Pseudomonas aeruginosa *Structure* **16** 1027–35

[32] Movileanu L, Schmittschmitt J P, Scholtz J M and Bayley H 2005 Interactions of the peptides with a protein pore *Biophys. J.* **89** 1030–45

[33] Hanggi P, Talkner P and Borkovec M 1990 Reaction-rate theory—50 years after Kramers *Rev. Mod. Phys.* **62** 251–341

[34] Andersen O S 1999 Graphic representation of the results of kinetic analyses *J. Gen. Physiol.* **114** 589–90

[35] Jordan P C 1999 Ion permeation and chemical kinetics *J. Gen. Physiol.* **114** 601–3

[36] Kang X F, Gu L Q, Cheley S and Bayley H 2005 Single protein pores containing molecular adapters at high temperatures *Angew Chem. Int. Edn Engl.* **44** 1495–9

[37] Jung Y, Bayley H and Movileanu L 2006 Temperature-responsive protein pores *J. Am. Chem. Soc.* **128** 15332–40

[38] Chimerel C, Movileanu L, Pezeshki S, Winterhalter M and Kleinekathofer U 2008 Transport at the nanoscale: temperature dependance of ion conductance *Eur. Biophys. J.* **38** 121–5

[39] Goodrich C P *et al* 2007 Single-molecule electrophoresis of β-hairpin peptides by electrical recordings and Langevin dynamics simulations *J. Phys. Chem.* B **111** 3332–5

[40] Hille B 2001 *Ion Channels of Excitable Membranes* 3rd edn (Sunderland, MA: Sinauer)

[41] Movileanu L, Neagoe I and Flonta M L 2000 Interaction of the antioxidant flavonoid quercetin with planar lipid bilayers *Int. J. Pharm.* **205** 135–46

[42] Movileanu L and Bayley H 2001 Partitioning of a polymer into a nanoscopic protein pore obeys a simple scaling law *Proc. Natl Acad. Sci. USA* **98** 10137–41

[43] Movileanu L, Cheley S, Howorka S, Braha O and Bayley H 2001 Location of a constriction in the lumen of a transmembrane pore by targeted covalent attachment of polymer molecules *J. Gen. Physiol.* **117** 239–51

[44] Movileanu L, Cheley S and Bayley H 2003 Partitioning of individual flexible polymers into a nanoscopic protein pore *Biophys. J.* **85** 897–910

[45] McManus O B, Blatz A L and Magleby K L 1987 Sampling, log binning, fitting, and plotting durations of open and shut intervals from single channels and the effects of noise *Pflugers Arch.* **410** 530–53

[46] McManus O B and Magleby K L 1988 Kinetic states and modes of single large-conductance calcium-activated potassium channels in cultured rat skeletal-muscle *J. Physiol.* **402** 79–120

[47] Kyte J and Doolittle R F 1982 A simple method for displaying the hydropathic character of a protein *J. Mol. Biol.* **157** 105–32
[48] Rubinstein M and Colby R 2003 *Polymer Physics* (Oxford: Oxford University Press)
[49] Scherer P O J and Fischer S F 2010 *Theoretical Molecular Biophysics* (Heidelberg: Springer)
[50] Niedzwiecki D J, Grazul J and Movileanu L 2010 Single-molecule observation of protein adsoption onto an inorganic surface *J. Am. Chem. Soc.* **132** 10816–22
[51] Maglia G, Restrepo M R, Mikhailova E and Bayley H 2008 Enhanced translocation of single DNA molecules through α-hemolysin nanopores by manipulation of internal charge *Proc. Natl Acad. Sci. USA* **105** 19720–5
[52] Zhao Q, Jayawardhana D A, Wang D and Guan X 2009 Study of peptide transport through engineered protein channels *J. Phys. Chem.* B **113** 3572–8
[53] Tian P and Andricioaei I 2005 Repetitive pulling catalyzes co-translocational unfolding of barnase during import through a mitochondrial pore *J. Mol. Biol.* **350** 1017–34
[54] Huang L, Kirmizialtin S and Makarov D E 2005 Computer simulations of the translocation and unfolding of a protein pulled mechanically through a pore *J. Chem. Phys.* **123** 124903
[55] Huang L and Makarov D E 2008 Translocation of a knotted polypeptide through a pore *J. Chem. Phys.* **129** 121107
[56] Kirmizialtin S, Ganesan V and Makarov D E 2004 Translocation of a β-hairpin-forming peptide through a cylindrical tunnel *J. Chem. Phys.* **121** 10268–77
[57] Kirmizialtin S, Huang L and Makarov D E 2006 Computer simulations of protein translocation *Phys. Status Solidi* b **243** 2038–47
[58] Makarov D E 2008 Computer simulations and theory of protein translocation *Acc. Chem. Res.* **42** 281–9